

has been inferred from selective broadening studies. The lack of quantitative correspondence between the  $T_{1P}$  and  $T_{2P}$  results renders suspect conclusions concerning the mode of interaction of paramagnetic ions and nucleic acid bases where only selective broadening experiments have been performed and a dipolar mechanism assumed. The  $T_{1P}$  results suggest that Cu(II) binds to both N1 and N7 of adenosine. Scalar interactions contribute to  $T_{2P}^{-1}$  and not to  $T_{1P}^{-1}$ . Table I indicates  $T_{1P}/T_{2P}$  is 1.6 times greater for H2 than H8 on AMP. Hence if equal binding were to occur at both N1 and N7 sites, H2 would exhibit greater broadening than H8, if only the effects of nearby Cu(II) are considered. However, analysis of unpaired spin densities at carbon atoms, such as those just made for imidazole also apply to nucleic acid bases, complicating greatly interpretations of selective broadening and even selective  $T_1$  experiments. On the basis of selective broadening experiments in aqueous solutions of 5'-AMP, a binuclear structure with two stacked nucleotides and two Cu(II) has been proposed.<sup>19</sup> These experiments were performed with large excesses of ligand over Cu(II), 2000/1 or even greater. If all the nucleotides are stacked in pairs, the probability of two Cu(II) occurring simultaneously on one pair is one part or less in  $10^6$ . Thus the binuclear structure proposed for stacked pairs of 5'-AMP and 3'-AMP in these solutions must be rejected. Relaxation time results for many Table I ligands with Mn(II) have also been obtained.<sup>20</sup>

**Acknowledgment.** We thank Professor Arthur S. Brill for helpful discussions. This research was supported by two

grants from the National Science Foundation, one from the molecular biology section and the other from the chemistry section for purchase of the NMR instrument.

## References and Notes

- (1) I. Solomon, *Phys. Rev.*, **99**, 559 (1955); N. Bloembergen, *J. Chem. Phys.*, **27**, 572, 595 (1957).
- (2) R. A. Dwek, R. J. P. Williams, and A. V. Xavier in "Metal Ions in Biological Systems", Vol. 4, H. Sigel, Ed., Marcel Dekker, New York, N.Y., 1974, Chapter 3.
- (3) T. J. Swift and R. E. Connick, *J. Chem. Phys.*, **37**, 307 (1962); **41**, 2553 (1964).
- (4) W. G. Espersen, W. C. Hutton, S. T. Chow, and R. B. Martin, *J. Am. Chem. Soc.*, **96**, 8111 (1974).
- (5) H. C. Freeman, *Adv. Protein Chem.*, **22**, 257 (1967).
- (6) R. B. Martin in ref 2, Vol. 1, Chapter 4.
- (7) J. T. Tsangaris and R. B. Martin, *J. Am. Chem. Soc.*, **92**, 4255 (1970).
- (8) N. C. Li, R. L. Scruggs, and E. D. Becker, *J. Am. Chem. Soc.*, **84**, 4650 (1962).
- (9) R. F. Pasternack, M. Angwin, and E. Gibbs, *J. Am. Chem. Soc.*, **92**, 5878 (1970).
- (10) P. J. Morris and R. B. Martin, *Inorg. Chem.*, **10**, 964 (1971).
- (11) M. Ihnat and R. Bersohn, *Biochemistry*, **9**, 4555 (1970).
- (12) R. J. Sundberg and R. B. Martin, *Chem. Rev.*, **74**, 471 (1974).
- (13) D. B. McCormick, H. Sigel, and L. D. Wright, *Biochim. Biophys. Acta*, **184**, 318 (1969).
- (14) W. B. Makinen, A. F. Pearlmutter, and J. E. Stuehr, *J. Am. Chem. Soc.*, **91**, 4083 (1969).
- (15) R. D. Allendoerfer and A. S. Pollock, *Mol. Phys.*, **22**, 661 (1971).
- (16) H. M. McConnell, *J. Chem. Phys.*, **24**, 632 (1956).
- (17) J. Eisinger, R. G. Shulman, and B. M. Szymanski, *J. Chem. Phys.*, **36**, 1721 (1962); B. P. Gaber, W. E. Schillinger, S. H. Koenig, and P. Aisen, *J. Biol. Chem.*, **245**, 4251 (1970).
- (18) M. Karpus and G. K. Fraenkel, *J. Chem. Phys.*, **35**, 1312 (1961).
- (19) N. A. Berger and G. L. Eichhorn, *Biochemistry*, **10**, 1847 (1971).
- (20) W. G. Espersen and R. B. Martin, *J. Phys. Chem.*, in press.

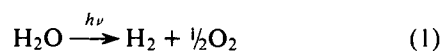
## Photoassisted Electrolysis of Water by Ultraviolet Irradiation of an Antimony Doped Stannic Oxide Electrode

Mark S. Wrighton,\*<sup>1</sup> David L. Morse, Arthur B. Ellis,<sup>2</sup> David S. Ginley,<sup>3</sup> and Harmon B. Abrahamson

Contribution from the Department of Chemistry, Massachusetts Institute of Technology, Cambridge, Massachusetts 02139. Received April 15, 1975

**Abstract:** Products, stoichiometry, and the stability of the photoelectrode show that the n-type semiconductor Sb-SnO<sub>2</sub>, as a single crystal, can serve as the photoreceptor in a photoelectrochemical cell to electrolyze H<sub>2</sub>O to H<sub>2</sub> and O<sub>2</sub>. The O<sub>2</sub> is evolved at the irradiated Sb-SnO<sub>2</sub> electrode, and the H<sub>2</sub> is evolved at the Pt electrode of the cell. Substantial photocurrents are obtained when the applied potential (+ lead to SnO<sub>2</sub>) exceeds ~0.5 V, and light of greater energy than the 3.5 eV band gap of SnO<sub>2</sub> is required to observe photoeffects at 25°. Importantly, increasing the temperature results in a measurable shift to lower energy for the onset of the photoeffects. The quantum efficiency for electron flow at 254 nm at 0.0 V vs. SCE in 1.0 M NaOH is 0.27 ± 0.03, and the wavelength response curve and current-voltage curve show that the quantum efficiency for electron flow is near unity at higher energy excitation wavelengths and slightly higher applied potentials. The photocurrent produces H<sub>2</sub> with >90% efficiency. Experiments with H<sub>2</sub><sup>18</sup>O show that the O<sub>2</sub> produced is not due to decomposition of SnO<sub>2</sub>, and additionally, stability of the SnO<sub>2</sub> photoelectrode has been determined by constant weight before and after prolonged irradiation.

Photoelectrochemical cells employing reduced TiO<sub>2</sub>, an n-type semiconductor, as the photoelectrode have recently been shown<sup>4</sup> to sustain the photoinduced electrolysis of H<sub>2</sub>O (reaction 1).



Strong interest in TiO<sub>2</sub><sup>4-10</sup> stems from the fact that it does not undergo decomposition upon illumination in an aqueous electrolyte. Such decomposition is common for several semiconductor photoelectrodes that have been investi-

gated.<sup>11</sup> The stability of TiO<sub>2</sub> has roused new hopes for the conversion of optical energy into chemical energy, and such photoassistance agents may also be used to carry out special chemical synthetic missions. In discussion<sup>12-14</sup> of the use of photoelectrochemical cells as solar energy conversion devices, it has been pointed out that TiO<sub>2</sub> is the only known semiconductor that is inert—a fact which may limit the usefulness of such systems. In this report we wish to outline our characterization of the photoassisted electrolysis of H<sub>2</sub>O using a second inert photoelectrode system: Sb-doped SnO<sub>2</sub>, an n-type semiconductor.

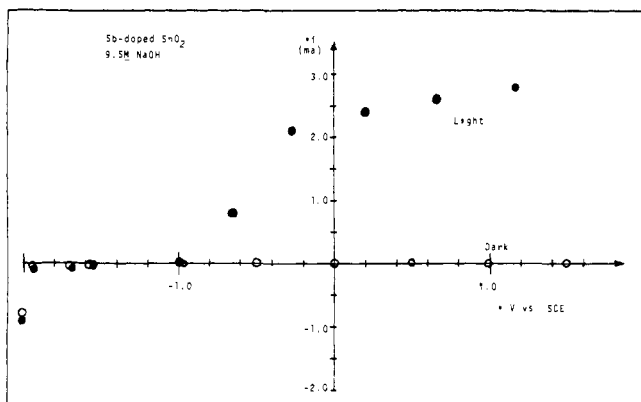


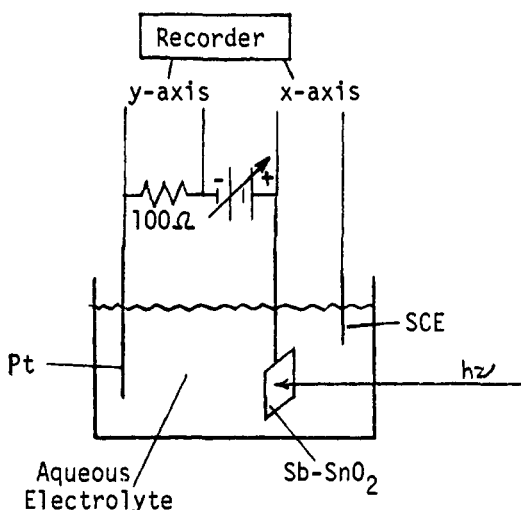
**Figure 1.** Current-voltage curve for Sb-SnO<sub>2</sub> (crystal III) in 12.0 M NaOH. The potential of the Sb-SnO<sub>2</sub> electrode is shown relative to the SCE with illumination (●) and in the dark (○). Positive currents correspond to O<sub>2</sub> evolution at the SnO<sub>2</sub> and negative current corresponds to the reduction of the SnO<sub>2</sub> and/or H<sub>2</sub> evolution at SnO<sub>2</sub>.

Some work has already been carried out on photoeffects on SnO<sub>2</sub> crystals<sup>15</sup> and SnO<sub>2</sub> polycrystalline films.<sup>16</sup> The prediction<sup>15</sup> that SnO<sub>2</sub> would be inert has not been proven, and the characterization of the SnO<sub>2</sub> photoelectrode system as a photoassistance agent for reaction 1 has not been reported. The band gap of SnO<sub>2</sub> is 3.5 eV,<sup>17</sup> or 0.5 eV higher than for TiO<sub>2</sub> which has a band gap of 3.0 eV.<sup>18</sup> Thus, the onset of response is likely to occur at shorter wavelengths for SnO<sub>2</sub> than for TiO<sub>2</sub>. However, the value of the present work rests in the demonstration that a material other than TiO<sub>2</sub> can be used as electrode material for the photo-assisted electrolysis of H<sub>2</sub>O. Moreover, some new principles and effects can emerge from studies of such materials. In particular, in this study we demonstrate a measurable temperature effect on the wavelength response of the photoelectrode.

## Results

Irradiation of the Sb-SnO<sub>2</sub> single-crystal electrode in a standard three-electrode electrochemical cell (Scheme I)

Scheme I



yields electron flow from the Sb-SnO<sub>2</sub> electrode towards the dark Pt electrode. The current-voltage curve upon illumination with ultraviolet light from a 200-W super high pressure Hg arc lamp is shown in Figure 1 for the Sb-SnO<sub>2</sub> that we designate as crystal III. The onset of the photoeffect is near -0.9 V vs. SCE in 12.0 M NaOH. In less alkaline solution the onset of the photocurrent is more positive,

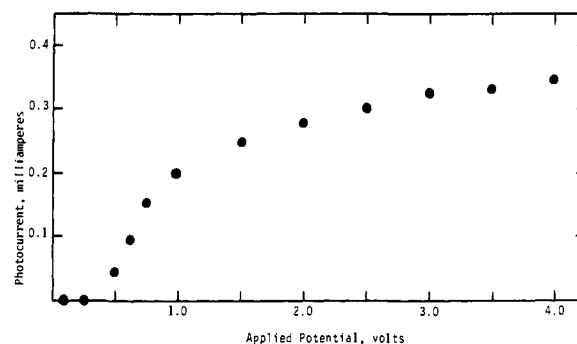


**Figure 2.** Decomposition current-voltage curve for Sb-SnO<sub>2</sub> (crystal III) in 12.0 M NaOH. Applied potential (+ lead to SnO<sub>2</sub>) against photocurrent is shown.

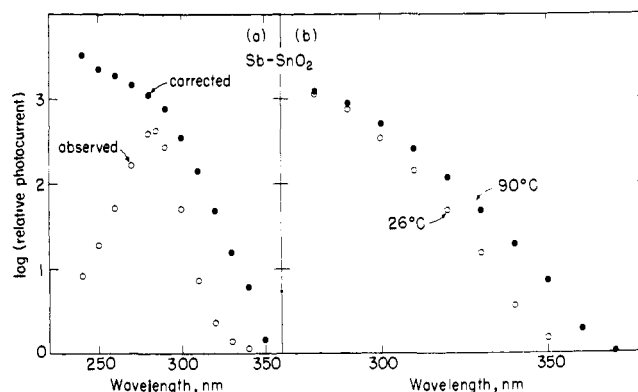


**Figure 3.** (a) Relative photocurrent as a function of the excitation wavelength for the Sb-SnO<sub>2</sub> electrode: (○) observed values; (●) corrected for variation in the intensity of the excitation source as a function of wavelength. (b) Corrected relative photoresponse of the Sb-SnO<sub>2</sub> crystal at 26°C (○) and 90°C (●).

consistent with the expected pH dependence.<sup>8a</sup> In discussing the efficiency of the photoelectrolysis it is appropriate to be aware of the photocurrent as a function of applied potential as shown in Figure 2. These data show that the onset of photocurrent occurs at a substantially lower applied potential than the 1.23 V thermodynamically required to electrolyze H<sub>2</sub>O.

At sufficiently high intensity irradiation gas evolution at both the Pt and SnO<sub>2</sub> electrode is obvious. Irradiation in 2.2 M NaOH in H<sub>2</sub><sup>18</sup>O/H<sub>2</sub>O (1/4) yields H<sub>2</sub> at the Pt electrode and a mixture of <sup>18</sup>O<sub>2</sub>, <sup>16</sup>O<sup>18</sup>O, <sup>16</sup>O<sub>2</sub> (0.04, 0.4, 1.0) at the Sb-SnO<sub>2</sub> electrode. Stoichiometric data in Table I show that the reaction is essentially that associated with the electrolysis of H<sub>2</sub>O. There is substantial deficiency in O<sub>2</sub> evolution in acidic or weakly alkaline solution, but generally the H<sub>2</sub> is found in amounts predicted by the integrated current. The O<sub>2</sub> deficiency is likely due to the production of H<sub>2</sub>O<sub>2</sub> which is not completely decomposed to O<sub>2</sub> and H<sub>2</sub>O near the electrode. Strong base catalyzes the H<sub>2</sub>O<sub>2</sub> decomposition and yields the best H<sub>2</sub>:O<sub>2</sub> ratios. No decomposition of the electrode could be detected by weight loss, Table II, confirming that the reaction is catalytic with respect to the electrode system. These measurements and product identification show that the n-type semiconductor SnO<sub>2</sub> photoreceptor (anode) and Pt (cathode) electrode system is a true photoassistance agent for the conversion of H<sub>2</sub>O to H<sub>2</sub> and O<sub>2</sub>. For periods up to 30 hr a photocurrent of ~3 mA has been shown to be constant within 10%.

Absorption measurements<sup>17</sup> have shown that the band gap in SnO<sub>2</sub> is 3.5 eV which corresponds to about 350-nm light. We find a sharp increase in photoeffect at the band gap energy, and, as seen in Figure 3a, the photosensitivity

Table I. Typical Stoichiometric Data for the SnO<sub>2</sub> Photoassisted Electrolysis of H<sub>2</sub>O<sup>a</sup>

Electrolyte	Crystal <sup>b</sup>	Potential of SnO <sub>2</sub> vs. SCE, V	Irrdn time, sec	Av current, <sup>c</sup> mA	Moles × 10 <sup>4</sup>		
					H <sub>2</sub>	O <sub>2</sub>	Electrons
1.0 M NaOH	III	0.0	17 100	1.04	0.74	0.12	1.84
1.0 M NaOH	III	+2.0	12 600	1.50	1.02	0.16	1.96
5.0 M NaOH	III	0.0	1 710	2.25	0.20	0.08	0.40
5.0 M NaOH	III	+1.82	5 400	3.10	0.82	0.35	1.73
5.0 M NaOH	III	0.0	9 360	0.94	0.44	0.19	0.91
5.0 M NaOH	III	+2.0	5 904	1.20	0.38	0.10	0.73
5.0 M NaOH	III	+2.0	9 360	2.60	1.26	0.43	2.52
6.8 M NaOH	III	0.0	15 550	2.20	1.80	0.78	3.63
12.0 M NaOH	III	0.0	25 060	1.29	1.72	0.82	3.35
1.0 M NaOH	II	+1.5	91 440	2.75	12.0	4.10	26.0
1.0 M NaOH	II	+0.5	67 680	1.42	4.06	1.38	9.94
1.0 M NaOH	II	+1.5	16 992	4.15	3.62	1.47	7.30
0.1 N H <sub>2</sub> SO <sub>4</sub>	I	+1.0	9 360	1.03	0.37	Not obsd	1.00
1.0 M NaOH	I	+0.5	98 640	0.88	3.70	0.71	9.01

<sup>a</sup> Irradiation of a Sb-SnO<sub>2</sub> photoelectrode from crystal I, II, or III using the 200-W superpressure Hg lamp source filtered with H<sub>2</sub>O (18 cm). The total output of the lamp was focused into the Sb-SnO<sub>2</sub> unless noted otherwise. <sup>b</sup> Crystals I and III are from the same crop of crystals and crystal II is from a different crop; cf. Experimental and Table II. <sup>c</sup> Determined by monitoring potential across a 100 Ω resistor.

Table II. Stability of the Sb-SnO<sub>2</sub> Photoelectrode<sup>a</sup>

Crystal	Moles of SnO <sub>2</sub>		Mol of O <sub>2</sub> photogenerated
	Before irrdrn	After irrdrn	
I	1.20 × 10 <sup>-3</sup>	1.17 × 10 <sup>-3</sup>	3.28 × 10 <sup>-4</sup>
II	6.64 × 10 <sup>-4</sup>	6.68 × 10 <sup>-4</sup>	6.95 × 10 <sup>-4</sup>

<sup>a</sup> Moles of SnO<sub>2</sub> in crystal before and after irradiation determined by weight and O<sub>2</sub> evolved in a photoelectrochemical cell as in Scheme I at ≤ 2.0 V applied potential in 1 M NaOH.

Table III. Quantum Efficiency for Electron Flow<sup>a</sup>

Potential of SnO <sub>2</sub> vs. SCE, V	φ <sub>313nm</sub> <sup>b</sup> ± 10%	φ <sub>254nm</sub> <sup>c</sup> ± 10%
-0.5	0.01 <sub>1</sub>	—
-0.3	0.04 <sub>1</sub>	—
0.0	0.05 <sub>1</sub>	0.27
+0.5	0.06 <sub>0</sub>	—
+1.0	0.06 <sub>9</sub>	—
+2.0	0.08 <sub>0</sub>	—

<sup>a</sup> Determined using crystal III from same crop as crystal I of Table II in 1.0 M NaOH using a photoelectrochemical cell as in Scheme I. <sup>b</sup> 1.77 × 10<sup>-9</sup> einstein/sec is the light intensity. <sup>c</sup> 9.83 × 10<sup>-10</sup> einstein/sec is the light intensity.

tends to level off above 250 nm. The response of the SnO<sub>2</sub> as a function of wavelength found here resembles the absorption curve<sup>17</sup> but differs somewhat from that of ref 15 where the photocurrent was found to decline at energies higher than ~320 nm. The wavelength response curve shown in Figure 3a has been corrected for variation in the intensity of the excitation light as a function of wavelength. Such a correction may not have been made in the earlier work.

Based on the general notion that the absorption edge in semiconductors red shifts with increasing temperature, we have investigated the wavelength response characteristics of SnO<sub>2</sub> as a function of temperature in the liquid range of water. Typical results are shown in Figure 3 which show that the "photoresponse edge" shifts noticeably to the red upon increasing the temperature from 26 to 90°C. As shown in Figure 4, the effect shows no sign of leveling off at 100°C, and is completely reversible with cooling. Similar temperature effects were found with two different crystals, and little or no temperature effect was found at 254 nm where the response has nearly leveled. Shifts in the absorption edge with temperature have been measured<sup>17</sup> and compare favorably with shifts found here.

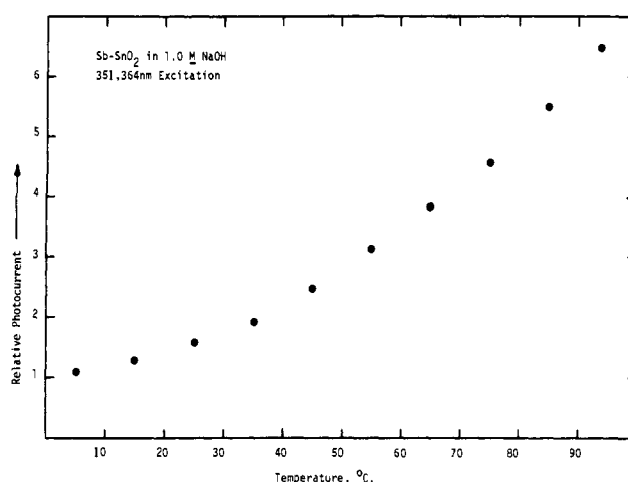


Figure 4. Temperature dependence of the photocurrent upon irradiation of the Sb-SnO<sub>2</sub> electrode with the 351, 364 nm doublet emission of an argon ion laser. No temperature dependence was found under the same conditions upon 254-nm irradiation.

We have determined the observed quantum efficiency for electron flow as a function of potential of the SnO<sub>2</sub> electrode relative to the SCE, Table III. The values are the number of electrons flowing per photon incident on the SnO<sub>2</sub> crystal in 1.0 M NaOH with a Pt wire cathode. The relative values at 313 and 254 nm are in good agreement with the wavelength response given in Figure 3a. The maximum quantum efficiency actually measured is 0.27 at 254 nm and 0.0 V vs. SCE in 1.0 M NaOH. However, 254 nm is not the wavelength of maximum photoeffect, and the maximum photoeffect does not obtain at 0.0 V vs. the SCE. It is apparent that at shorter excitation wavelengths and higher applied potentials the quantum efficiency will be nearly unity.

## Discussion

The results show unequivocally that the Sb-SnO<sub>2</sub> photoelectrode system will photoassist the electrolysis of H<sub>2</sub>O with external applied potentials of less than 1.23 V. In comparing the present system to the TiO<sub>2</sub> photoelectrode<sup>4</sup> system it is appropriate to consider stability, stoichiometry, quantum efficiency, current-voltage properties, and wavelength response.

For both TiO<sub>2</sub> and SnO<sub>2</sub> there seem to be no problems associated with electrode decomposition under positive bias

and intense, prolonged irradiation. Each system responds to light of energy greater than the band gap energy, and consequently, the  $\text{SnO}_2$  emerges as less efficient at room temperature having a band gap of 3.5 eV<sup>17</sup> vs. 3.0 for  $\text{TiO}_2$ .<sup>18</sup> Importantly, though, we have established that even in the liquid range of  $\text{H}_2\text{O}$  at normal conditions we can increase the low energy response of  $\text{SnO}_2$  by increasing the temperature. Admittedly, the effects we find are small in an absolute sense, but the measurements herein do establish the principle. It is worth noting that unreduced  $\text{TiO}_2$  undergoes reversible electronic absorption spectral changes with temperature variations such that the absorption edge moves substantially into the visible region with increases in temperature.<sup>18</sup> Aside from the red-shifted response of the photoelectrode as the temperature is increased, the potential required for the electrolysis of  $\text{H}_2\text{O}$  decreases and overvoltages become less severe. Given that an elevated temperature is likely to be useful, solar energy can be more efficiently utilized since one can use the near-ir irradiation to raise the cell to an elevated temperature.

Though the maximum quantum efficiency for electron flow and stoichiometry for the  $\text{H}_2\text{O}$  electrolysis for  $\text{Sb-SnO}_2$  and  $\text{TiO}_2$ <sup>4</sup> are comparable, the current-voltage properties reported for  $\text{TiO}_2$ <sup>5,8a</sup> are somewhat superior to those reported here for the  $\text{Sb-SnO}_2$ . The key point is that in order to achieve photoelectrolysis an applied potential is required, but compared to  $\text{TiO}_2$  the  $\text{SnO}_2$  requires a slightly larger potential to achieve the onset of photocurrents corresponding to the electrolysis of  $\text{H}_2\text{O}$ . With the  $\text{SnO}_2$  photoelectrode there appears to be a base strength effect on the stoichiometry for the electrolysis. The evolution of  $\text{H}_2\text{O}_2$ , a high energy material, would obviously increase the energy conversion efficiency of the photoelectrochemical cells since the overall reaction is more endothermic. Small amounts of the  $\text{H}_2\text{O}_2$  were also detected from the  $\text{TiO}_2$  system.<sup>4</sup> This energetic consideration and the finding that photocurrents at zero applied potential for the  $\text{TiO}_2$  system<sup>4,6,7</sup> do not correspond to the electrolysis of  $\text{H}_2\text{O}$  show the importance of stoichiometric data of the type reported here.

## Summary

Except for wavelength response the  $\text{SnO}_2$  photoelectrode system is quite comparable to the  $\text{TiO}_2$  system for the photoassisted electrolysis of  $\text{H}_2\text{O}$ . The temperature effects on wavelength response and the medium effects on stoichiometry represent new aspects of the characterization of photoelectrochemical cells which may lead to more efficient optical to chemical energy conversion devices.

## Experimental Section

**Electrodes and Electrochemical Cell.** The Pt electrode was simply a Pt wire about 50 mm long and 1 mm in diameter, and the saturated calomel electrode (SCE) was obtained commercially. Twinned crystals of Sb-doped  $\text{SnO}_2$  were given to us by Professor C. G. Fonstad of M.I.T. for use in the photoelectrodes. The  $\text{Sb-SnO}_2$  crystals actually used are those whose synthesis and characteristics have already been described.<sup>19</sup> Three different  $\text{Sb-SnO}_2$  crystals were actually used: crystal I (~0.18 g) irradiated surface area  $\approx 2.5 \times 2.5$  mm; crystal II (~0.10 g); and crystal III (~0.50 g) irradiated surface area  $\approx 4 \times 2.5$  mm. None of these crystals had flat uniform surfaces. The resistivities for the crystals had been determined<sup>19</sup> to be of the order of 0.1 ohm cm with carrier concentrations of the order of  $4 \times 10^{17}$  cm<sup>-3</sup>. Crystals I and III are from the same crop, and crystal II is from a different crop (no substantial differences were found in their photoelectrochemical behavior). To prepare the photoelectrode a copper wire was attached to the  $\text{Sb-SnO}_2$  using conducting silver epoxy. The copper wire and silver epoxy were then insulated using ordinary epoxy and the wire and crystal were then mounted in a glass tube to maintain rigidity. The Pt, SCE, and photoelectrode were then placed in a circuit as shown in Scheme I.

The variable power supply was a Hewlett-Packard Model 6241 A, and the current and potential were measured with a Hewlett-Packard 7044A x-y recorder. The current was actually measured by monitoring the potential across a 100  $\Omega$  resistor in series with the electrodes. The electrolyte and electrodes were placed in a Vycor beaker. The gases,  $\text{H}_2$  and  $\text{O}_2$ , were typically collected in inverted graduated cylinders filled with the electrolyte. The 10- or 25-ml graduated cylinders were placed immediately above the electrodes, and only the gas produced near the electrodes was collected.

Mass spectroscopic measurements were carried out using a sealed, evacuated, cell in the shape of a U-tube. Prior to irradiation the electrolyte was purged with Ar. The Pt and  $\text{SnO}_2$  electrodes were on either side of the U and the gases evolved upon irradiation were collected in the two sampling devices attached at the top of the U. The gases were analyzed on a Hitachi-Perkin-Elmer RMU-6 mass spectrometer.

**Irradiations.** Typical irradiations were carried out using a Bausch and Lomb Hg lamp source equipped with an Osram 200-W super high pressure Hg lamp. The lamp was always filtered with an 18-cm path length of  $\text{H}_2\text{O}$  to remove a large fraction of the near-ir irradiation. The total output from the lamp was focused onto the photoelectrode. For quantum efficiency determinations at 313 nm, the  $\text{H}_2\text{O}$  filter solution was replaced with an aqueous  $1.2 \times 10^{-4}$  M  $\text{K}_2\text{Cr}_2\text{O}_7$  solution and a Corning 7-54 glass filter to isolate the 313-nm Hg emission. The 254-nm quantum efficiency was determined using an Ultraviolet Products, Inc., low pressure Hg lamp as the excitation source. Light intensity was measured by ferrioxalate actinometry.<sup>20</sup> In the quantum efficiency determinations only the light that was striking the electrode was actually measured by the actinometer, but the quantum efficiency values reported have not been corrected for reflection or incomplete absorption of the incident light by the  $\text{Sb-SnO}_2$  crystal.

To determine the wavelength response of  $\text{Sb-SnO}_2$  photoelectrodes the excitation optics of an Aminco-Bowman SPF-2 were used to provide the monochromatic excitation light in the 240–400-nm range. The relative intensity of the light as a function of the wavelength was determined using a rhodamine B quantum counter.<sup>21</sup>

The temperature dependence of the photocurrent at the absorption edge was conveniently studied using the doublet 351, 364 nm emission from a Spectra Physics Model 164 Argon ion laser at 20–40 mW as the excitation source. The temperature dependence was determined twice for crystals I and III and found to be nearly the same. No temperature dependence was found using 254-nm excitation.

**Acknowledgment.** We acknowledge the National Aeronautics and Space Administration for support of this research, and we thank Professor C. G. Fonstad for the  $\text{Sb-SnO}_2$  crystals and several valuable discussions.

## References and Notes

- (1) Fellow of the Alfred P. Sloan Foundation, 1974–1976.
- (2) Fellow of the Fannie and John Hertz Foundation.
- (3) Uniroyal Fellow, Department of Chemistry, M.I.T., 1974–1975.
- (4) M. S. Wrighton, D. S. Ginley, P. T. Wolczanski, A. B. Ellis, D. L. Morse, and A. Linz, *Proc. Nat. Acad. Sci. U.S.A.*, **72**, 1518 (1975).
- (5) A. Fujishima and K. Honda, *Nature (London)*, **238**, 37 (1972), and *Bull. Chem. Soc. Jpn.*, **44**, 1148 (1971).
- (6) J. Keeney, D. H. Weinstein, and G. M. Haas, *Nature (London)*, **253**, 719 (1975).
- (7) W. Gissler, P. L. Lensi, and S. Pizzini, *J. Appl. Electrochem.*, in press.
- (8) (a) K. L. Hardee and A. J. Bard, *J. Electrochem. Soc.*, **122**, 739 (1975); (b) S. N. Frank and A. J. Bard, submitted for publication and private communication; (c) A. J. Nozik, *Nature (London)*, **257**, 383 (1975).
- (9) F. Möllers, H. J. Tolle, and R. Memming, *J. Electrochem. Soc.*, **121**, 1160 (1974).
- (10) H. Yoneyama, H. Sakamoto, and H. Tamura, *Electrochim. Acta*, **20**, 341 (1975).
- (11) (a) H. Gerischer and W. Mindt, *Electrochim. Acta*, **13**, 1239 (1968). (b) For a general discussion of semiconductor electrochemistry cf. V. A. Myamlin and Yu. V. Pleskov, "Electrochemistry of Semiconductors", Plenum Press, New York, N.Y., 1967, and H. Gerischer in "Physical Chemistry", Vol. IXA, H. Eyring, D. Henderson, and W. Jost, Ed., Academic Press, New York, N.Y., 1970, Chapter 5.
- (12) H. Gerischer, *J. Electroanal. Chem.*, **58**, 263 (1975).
- (13) M. D. Archer, *J. Appl. Electrochem.*, **5**, 17 (1975).
- (14) S. N. Paleocrassas, *Sol. Energy*, **16**, 45 (1974).
- (15) F. Möllers and R. Memming, *Ber. Bunsenges. Phys. Chem.*, **76**, 469 (1972).

- (16) H. Kim and H. A. Laitinen, *J. Electrochem. Soc.*, **122**, 53 (1975).  
 (17) M. Nagasawa and S. Shionoya, *J. Phys. Soc. Jpn.*, **30**, 1118 (1971).  
 (18) D. C. Cronmeyer, *Phys. Rev.*, **87**, 876 (1952).  
 (19) C. G. Fonstad, A. Linz, and R. H. Rediker, *J. Electrochem. Soc.*, **116**, 1269 (1969).  
 (20) C. G. Hatchard and C. A. Parker, *Proc. R. Soc., Ser. A*, **235**, 518 (1956).  
 (21) W. H. Melhuish, *J. Opt. Soc. Am.*, **52**, 1256 (1962).

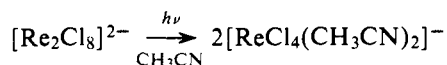
## Flash Kinetic Spectroscopy of $\text{Re}_2\text{Cl}_8^{2-}$ and $\text{Re}_2\text{Br}_8^{2-}$

R. H. Fleming,<sup>1a</sup> G. L. Geoffroy,<sup>1b</sup> Harry B. Gray,<sup>\*1c</sup> A. Gupta,<sup>1a</sup>  
 G. S. Hammond,<sup>1a</sup> D. S. Kliger,<sup>1a</sup> and V. M. Miskowski<sup>1a</sup>

*Contribution from the Division of Natural Sciences, University of California, Santa Cruz, California 95060, from the Department of Chemistry, Pennsylvania State University, University Park, Pennsylvania 16802, and No. 5013 from the Arthur Amos Noyes Laboratory of Chemical Physics, California Institute of Technology, Pasadena, California 91125. Received May 1, 1975*

**Abstract:** Laser flash photolysis studies of  $\text{Re}_2\text{Cl}_8^{2-}$  have revealed the presence of a short-lived transient (average  $\tau(\text{CH}_3\text{CN}) = 134$  nsec,  $\tau(\text{CH}_2\text{Cl}_2) = 73$  nsec). The same transient is observed upon 337 and 615 nm excitation. The transient exhibits an absorption maximum at 390 nm ( $\epsilon \geq 7.5 \times 10^3$ ). Kinetic data indicate that the transient is an electronic excited state of  $\text{Re}_2\text{Cl}_8^{2-}$ , most probably that corresponding to the  $\sigma^2\pi^4\delta^1(\delta^*)^1$  configuration. The 390-nm band is assigned to an  $e_u(\text{Cl}) \rightarrow \delta$  charge-transfer transition. The analogous transient of  $\text{Re}_2\text{Br}_8^{2-}$  (average  $\tau(\text{CH}_2\text{Cl}_2) = 51$  nsec) exhibits two  $e_u(\text{Br}) \rightarrow \delta$  charge-transfer bands, at 490 and 555 nm. For  $\text{Re}_2\text{Cl}_8^{2-}$ , only 80% of the excitation energy at 337 nm is internally converted to the  $\sigma^2\pi^4\delta^1(\delta^*)^1$  state. It is proposed that the remaining 20% of the upper excited states undergoes nonradiative decay to a halide-bridged intermediate, and that this pathway is the source of the photocleavage of  $\text{Re}_2$  in acetonitrile.

It has been shown recently that uv irradiation of  $[n\text{-Bu}_4\text{N}]_2[\text{Re}_2\text{Cl}_8]$  in acetonitrile solution results in cleavage of the quadruple  $\text{Re}_2$  bond and generation of monomeric  $[n\text{-Bu}_4\text{N}][\text{ReCl}_4(\text{CH}_3\text{CN})_2]^-$



The photoreaction has a marked wavelength dependence, with increasing quantum yields according to 366 (0.0065) < 313 (0.017) < 254 (0.045) nm.<sup>2,3</sup> Interestingly, irradiation into the least energetic absorption band (680 nm) gives no photoreaction, which establishes that bond cleavage derives from one or more of the higher energy excited states.<sup>2</sup>

The exact mechanism of the photoreaction is not known. It is reasonable to suppose that in the active excited state the dimer dissociates into two  $\text{ReCl}_4^-$  fragments, which subsequently react with  $\text{CH}_3\text{CN}$  to give the final product. Alternatively,  $\text{CH}_3\text{CN}$  molecules could bind to the excited dimer and assist the fragmentation reaction. It was felt that nanosecond flash photolysis studies of  $\text{Re}_2\text{Cl}_8^{2-}$  in  $\text{CH}_3\text{CN}$  and  $\text{CH}_2\text{Cl}_2$  (a solvent in which no net reaction occurs) would be useful in resolving this uncertainty, as inferences could then be made about the nature of any observed intermediates.

### Experimental Section

The flash photolysis apparatus used either a pulsed nitrogen laser or a dye laser as an excitation source and a xenon flashlamp as a monitoring source. The  $\text{N}_2$  laser was a Moletron UV-1000. It produced a pulse of 337-nm light with a duration of 10 nsec. The dye laser (a solution of Rhodamine B in ethanol, pumped by the  $\text{N}_2$  laser) produced a pulse of 615-nm light with a 10-nsec duration. The  $\text{N}_2$  and dye lasers delivered  $1.08 \times 10^{16}$  and  $2.6 \times 10^{15}$  photons per pulse, respectively, to the samples. The flashlamp produced a 3- $\mu\text{sec}$  pulse of white light for monitoring transient absorptions. Both the laser and the monitoring flashes were focused down to ellipses of area approximately 0.25  $\text{cm}^2$  on the samples. The detection system consisted of a Bausch and Lomb 0.25-m monochromator and a 1 P28 photomultiplier whose output was mea-

sured on a Tektronix 475 oscilloscope (1.4 nsec rise time). Solutions were  $10^{-3}$  to  $10^{-2}$  M in the tetrabutylammonium salts of  $\text{Re}_2\text{Cl}_8^{2-}$  and  $\text{Re}_2\text{Br}_8^{2-}$ , and were either rigorously degassed by three to four freeze-pump-thaw cycles or were saturated with  $\text{O}_2$ .

### Results and Discussion

Flash photolysis of  $\text{Re}_2\text{Cl}_8^{2-}$  in  $\text{CH}_3\text{CN}$  and  $\text{CH}_2\text{Cl}_2$  solutions produces the transient electronic absorption spectra shown in Figures 1 and 2, respectively. In both solvents the transient shows an absorption maximum at 390 nm. By using the known excitation source intensity and assuming that one photon at 615 nm produces one transient molecule, we calculate  $\epsilon_{390} \geq 7.5 \times 10^3$ . Lifetime data are given in Table I. First-order kinetic plots are strictly linear at all wavelengths, evidencing a single transient. Further, the similarity of the absorption spectra obtained upon 337 and 615 nm excitation in  $\text{CH}_3\text{CN}$  and  $\text{CH}_2\text{Cl}_2$  indicates that the same transient is produced in all cases.

The transient observed is in all probability an excited state of  $\text{Re}_2\text{Cl}_8^{2-}$ . If it were a dissociated fragment, such as  $\text{ReCl}_4^-$ , it could not decay by first-order kinetics in dichloromethane, where the quantum yield for photoreaction is vanishingly small,<sup>3</sup> nor could it do so in acetonitrile, where we estimate the quantum yield for production of the absorbing transient to be 0.8 for 337-nm excitation (vide infra), as compared with a quantum yield of 0.017 for  $\text{Re}_2$  photocleavage.<sup>2</sup> The short transient lifetimes of 73 nsec in  $\text{CH}_2\text{Cl}_2$  and 134 nsec in  $\text{CH}_3\text{CN}$  are also consistent with this species being an electronic excited state of  $\text{Re}_2\text{Cl}_8^{2-}$ . As the least energetic electronic transition (centered at 680 nm in the ground state complex) has been shown<sup>4</sup> to be  $\delta \rightarrow \delta^*$ , the most reasonable candidate for the transient is an excited state with a  $\sigma^2\pi^4\delta^1(\delta^*)^1$  electronic configuration in the  $\text{Re}_2$  bond framework. The absence of a large solvent effect on the excited state absorption spectrum conclusively shows that neither  $\text{CH}_3\text{CN}$  nor  $\text{CH}_2\text{Cl}_2$  coordinates directly to  $\sigma^2\pi^4\delta^1(\delta^*)^1 \text{Re}_2\text{Cl}_8^{2-}$ .<sup>5</sup>

We observe only marginally significant quenching of the